Applied Physics Letters

RESEARCH ARTICLE | OCTOBER 16 2023

Cryogenic packaging of nanophotonic devices with a low coupling loss <1 dB

Beibei Zeng ; Chawina De-Eknamkul ; Daniel Assumpcao ; Dylan Renaud ; Zhuoxian Wang ; Daniel Riedel; Jeonghoon Ha ; Carsten Robens ; David Levonian ; Mikhail Lukin; Ralf Riedinger ; Mihir Bhaskar ; Denis Sukachev; Marko Loncar; Bart Machielse

Appl. Phys. Lett. 123, 161106 (2023)
https://doi.org/10.1063/5.0170324

AIP Publishing

Applied Physics Letters ARTICLE pubs.aip.org/aip/apl

Cryogenic packaging of nanophotonic devices with a low coupling loss <1 dB

Cite as: Appl. Phys. Lett. **123**, 161106 (2023); doi: 10.1063/5.0170324
Submitted: 2 August 2023 · Accepted: 30 September 2023 ·
Published Online: 16 October 2023

Beibei Zeng,[1] Chawina De-Eknamkul,[1] Daniel Assumpcao,[2] Dylan Renaud,[2] Zhuoxian Wang,[1] Daniel Riedel,[1] Jeonghoon Ha,[1] Carsten Robens,[1] David Levonian,[1] Mikhail Lukin,[3] Ralf Riedinger,[4] Mihir Bhaskar,[1] Denis Sukachev,[1] Marko Loncar,[2] and Bart Machielse[1,a)]

AFFILIATIONS

[1]AWS Center for Quantum Networking, Boston, Massachusetts 02135, USA
[2]John A. Paulson School of Engineering and Applied Sciences, Harvard University, Cambridge, Massachusetts 02138, USA
[3]Department of Physics, Harvard University, Cambridge, Massachusetts 02138, USA
[4]Institut für Laserphysik und Zentrum für Optische Quantentechnologien, Universität Hamburg, 22761 Hamburg, Germany

[a)]**Author to whom correspondence should be addressed:** machiel@amazon.com

ABSTRACT

Robust, low-loss photonic packaging of on-chip nanophotonic circuits is a key enabling technology for the deployment of integrated photonics in a variety of classical and quantum technologies including optical communications and quantum communications, sensing, and transduction. To date, no process has been established that enables permanent, broadband, and cryogenically compatible coupling with sub-dB losses from optical fibers to nanophotonic circuits. Here, we report a technique for reproducibly generating a permanently packaged interface between a tapered optical fiber and nanophotonic devices on diamond with a record-low coupling loss <1 dB per facet at near-infrared wavelengths ($\sim$730 nm) that remains stable from 300 K to 30 mK. We further demonstrate the compatibility of this technique with etched lithium niobate on insulator waveguides. The technique lifts performance limitations imposed by scattering as light transfers between photonic devices and optical fibers, paving the way for scalable integration of photonic technologies at both room and cryogenic temperatures.

Low-loss optical interfaces are crucial for optical information transport and processing across photonic and optoelectronic technologies. For instance, efficient light coupling between optical fibers and on-chip waveguides in photonic integrated circuits (PICs) has enabled numerous applications in optical/quantum interconnects,[1,2] optical switches,[3] nonlinear optics,[4] and quantum photonics.[5,6] In particular, quantum information technologies rely on coherent control over interactions of single photons and qubits, which depend sharply on efficient transfer of quantum states of photons in and out of quantum PICs.[7] Significant progresses have been made in the chip-scale manipulation of photonic qubits for integrated quantum technologies,[8] including all-optical quantum computing employing cluster states,[9] quantum sensing,[10] and quantum communication.[11,12] However, scalable implementation of solid-state quantum computation[13] and communication[11,12] platforms has been prevented by the long-standing challenge of efficiently and reliably transferring photons in and out of quantum PICs at cryogenic temperatures, which are required to maintain high-fidelity quantum operations. This is extremely challenging because optical coupling interfaces made of heterogeneous materials experience thermal expansion mismatch as systems cool to the cryogenic temperatures, which imposes a fundamental trade-off between coupling efficiency and stability at the interface of optical fibers and quantum PICs, limiting the effectiveness and reliability of these devices.

A variety of technologies are being studied to enable efficient, cryogenically compatible photon transfer between optical fibers and PICs for scalable quantum technologies, but two technologies have emerged as dominant: edge coupling and grating coupling. Edge coupling between optical fiber and on-chip waveguide is accomplished by guiding an on-chip waveguide to the edge of the sample and launching the optical mode into free space, from where it can be collected into a carefully aligned optical fiber. This technique has demonstrated high coupling efficiency with less than 0.5 dB of loss[14] but is limited by its sensitivity to spatial alignment accuracy, which can be disrupted by the thermal expansion mismatch during thermal cycles and mechanical vibrations.[15,16] Thus, *in situ* optical alignment is typically required to achieve relatively high coupling efficiency at cryogenic temperatures.[16–19]

Recently, a cryogenically stable optical packaging for diamond nanophotonic devices without *in situ* alignment has been demonstrated.[20] However, in this demonstration, coupling loss between the optical fiber and the quantum device is limited to roughly 10 dB at visible wavelengths. For more established material platforms, such as SiN and Si, the coupling loss is ∼2.5 dB in the state-of-the-art cryogenically packaged devices.[15] On the other hand, grating couplers coherently scatter light from an on-chip waveguide into free-space using a periodically patterned grating such that it can be collected by an optical fiber. This technique has comparably higher tolerance to spatial alignment variations and has been utilized to package nanophotonic devices with the required stability at cryogenic temperatures.[21–23] Because of the large contact area between fiber and device and the relatively relaxed alignment tolerance, the optical coupling of packaged fiber–grating interface remains stable over many thermal cycles from room temperature (300 K) to 7 mK in a dilution refrigerator. Unfortunately, grating couplers generally suffer from narrow optical bandwidth and limited coupling efficiency due to optical mode mismatch and grating directionality, resulting in a roughly 5 dB coupling loss per facet from an optical fiber to a silicon optomechanical crystal at telecom wavelengths.[22]

In this work, we address this long-standing challenge by achieving a highly efficient fiber-chip coupling interface in a permanent, cryogenically compatible package. Our approach builds on the less established technology of adiabatic coupling,[24] which utilizes a smoothly transitioning interface between tapered optical fibers and tapered waveguides to adiabatically match optical modes between these two devices. Using active alignment inside cryostats, this technique has demonstrated a low coupling loss of ∼0.2 dB between optical fiber and nanophotonic waveguide with broad bandwidths.[12,24–27] This exceptionally low loss makes it suitable for quantum applications where photon loss between quantum devices can quickly deteriorate performance.[2,7,12] Previously, *in situ* alignment with complex nanopositioning stages and cryo-compatible imaging systems was required in this platform to compensate for thermal expansion mismatch, vibration induced shifts, and power-dependent instabilities at the optical coupling interface during thermal cycles, limiting the number of optical channels and increasing the system complexity and footprint. In order to eliminate the *in situ* alignment process, here we demonstrate highly efficient and permanent packaging of the optical interface between a tapered optical fiber and diamond nanophotonic devices with a coupling loss of <1 dB per facet. The packaged nanophotonic device is cryogenically stable, surviving more than five thermal cycles down to 77 K with an efficiency change of less than 0.15 dB. It is resistant to sudden thermal shocks, high-power illumination, and mechanical vibrations, enabling gas deposition based tuning and laser back-tuning of the resonance wavelength of the nanophotonic cavity inside in a dilution refrigerator.[12] Gas tuning can thus be used for individual targeting of cavity resonances to quantum emitters, facilitating the operation of a nanocavity integrated quantum memory. This technique is reproducible and compatible with multiple PIC platforms, including suspended diamond waveguides and thin film lithium niobate devices. Finally, in contrast to previously established techniques, this approach does not use adhesive at the point of contact between the fiber and waveguide device.

Figure 1(a) shows the schematic of our packaging approach. For most of the demonstrations in this paper, we choose as our target device a free-standing diamond waveguide optimized for efficient photon exchange with silicon vacancy color centers.[12,26,27] The diamond device has a photonic crystal cavity that acts as a reflector away from its cavity resonance and a tapered waveguide end used to create an adiabatic coupling interface with a tapered fiber.[25–27] The waveguide taper narrows from the waveguide width, 500 to 100 nm over 20 μm distance. The fiber taper is made from a single mode S630-HP optical fiber (3.5 μm core and 125 μm cladding diameters) by chemical etching in hydrofluoric acid.[25] Withdrawing the fiber from the etchant bath at a constant speed tapers the diameter of the fiber down to ∼150 nm at the fiber tip with a taper angle of about 1.5°. In simulations, the coupling loss between optical fiber and waveguide remains below 0.4 dB for a wide variety of alignment parameters, as shown in Fig. 1(b). Changes in the overlap between the fiber and waveguide tapers of less than 40 μm (out of a total overlap distance of less than 60 μm) cause coupling fluctuations of only 0.2 dB, and transverse translation only modestly impacts coupling efficiency as long as the tapered ends remain in contact (see the supplementary material). This waveguide–fiber interface is facilitated by strong van der Waals interactions, ensuring that once contact is made, it can easily be maintained.

The alignment and assembly setup shown in Fig. 2(a) consists of motorized translation stages for fiber alignment, an optical microscope

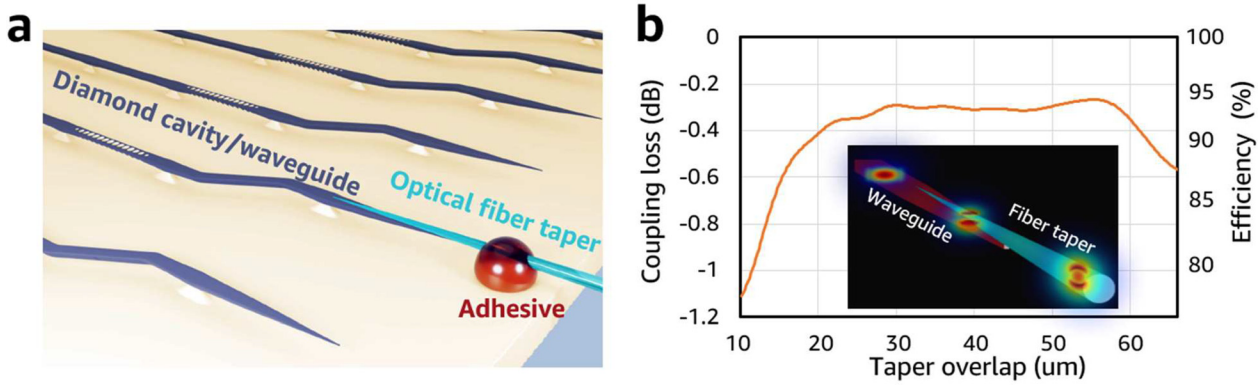

FIG. 1. (a) Illustration of the fiber-to-chip packaging concept. (b) Simulated coupling loss as a function of the taper overlap of an adiabatic interface between a tapered waveguide and fiber taper. Inset: optical mode fields at different locations along the coupling interface.

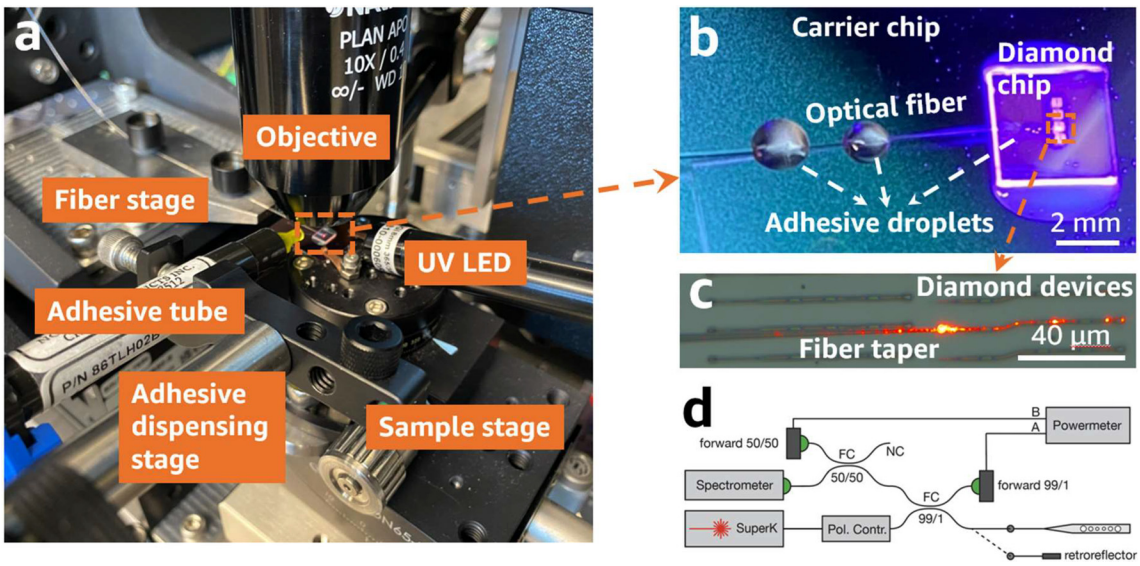

FIG. 2. (a) Customized alignment and assembly bench for fiber manipulation and gluing. (b) Fiber-packaged device on a 20 × 15 mm^2 SiN on Si carrier chip under UV illumination showing a series of adhesive droplets. (c) Optical image of fiber-coupled diamond nanophotonic device and (d) fiber network for coupling loss measurements.

for imaging, an optical coupling loss measurement system, an adhesive dispenser, and a UV curing station. Once the fiber is aligned and coupled to the optical device, as observed using optical images in Fig. 2(c) and verified using the measured reflection off the photonic crystal in Fig. 2(d), an adhesive (Norland NOA 86TLH) droplet is placed ∼200 μm away from the waveguide–fiber interface with a high-precision air-pumped adhesive dispenser (Nordson Ultimus V High Precision Dispensers), which can regulate and control the droplet diameter down to ∼150 μm. The adhesive is immediately UV cured to prevent flow, and more adhesive droplets are placed further down the fiber to secure the pigtail, as shown in Fig. 2(b). We further UV cure the package for several hours to fully polymerize the adhesive. Once cured, the sample can be handled, transported, installed in vacuum chambers, and cooled down without specialized handling. After initial optimization of this procedure, we packaged five successive devices with no process failures, reaching coupling efficiencies limited primarily by diamond device properties.

We note the surprising fact that the fiber tip is held in contact purely through the use of van der Waals (vdW) forces and not through the application of adhesive to the point of contact between the device and the fiber. Using this technique, we can create a stable, clean interface between optical waveguides in two different materials without consideration of the optical properties of adhesives used during the packaging process, as the optical mode is kept far from the adhesives.

This procedure has a number of advantages over the state-of-the-art photonic packaging techniques.[20–23] First, the measured change in insertion loss before and after gluing is negligible. This is because adhesive is far away from the point of contact and thus has a minimal impact on the coupling efficiency at the sensitive optical interface between fiber and waveguide. Such coupling efficiency is limited by the light scattering at the waveguide–fiber interface, not the packaging process added afterward. Second, this technique enables multiple fibers to be attached to a single chip, as there is minimal crosstalk between the attachment and curing of multiple interfaces. Finally, this approach does not require the use of valuable chip-edge space, as the fiber arrives at an angle of approximately 3° and thus does not contact substrate at any point past the first adhesive droplet, which is located ∼1.5 mm to the edge of diamond chip. This means that the chip edge real estate can be reserved for other optical and electronic interconnects and the density of interconnects on the chip can be increased.

To test the cryogenic stability of our packaged devices, we place each fiber-packaged device in a liquid nitrogen (LN2) flow cryostat as shown in Fig. 3(a). Because the coefficient of thermal expansion of materials drops at low temperatures, contraction mainly occurs between room temperature and 77 K.[22,23,28] This means that cooling to LN2 temperature provides a good indicator of the device performance at sub-Kelvin temperatures. We monitor the coupling efficiency in real time by connecting a cryostat feedthrough fiber to the fiber network in Fig. 2(d). To start a thermal cycle, we mount the sample inside the sample chamber on a copper pedestal using a conductive silver paste to ensure thermalization. The sample chamber is pumped down with a turbo pump station to a base pressure of less than 10^{-4} mbar. Then, we cool the sample at a rate of 3–4 K/min. To avoid optical tweezing of material freed from the cryochamber walls during cooldown, the laser is kept off until the temperature reaches 160 K. At this temperature, the laser is turned on, 20 μW of power is sent to the waveguide, and the intensity of the reflected light is monitored. We then keep the temperature constant at 77 K for an additional 30 minutes to allow the system to fully thermalize.

Figure 3(b) shows the real-time coupling loss of a packaged device during one such thermal cycle. For this sample, once the laser is turned on, the reflected power remained steady at ∼83% of the reference reflected power (Sec. 3 in the supplementary material). This quantity includes losses from two passes through the waveguide–fiber interface, reflection off the photonic crystal, and propagation through roughly 150 μm of diamond waveguide. By taking the square root of

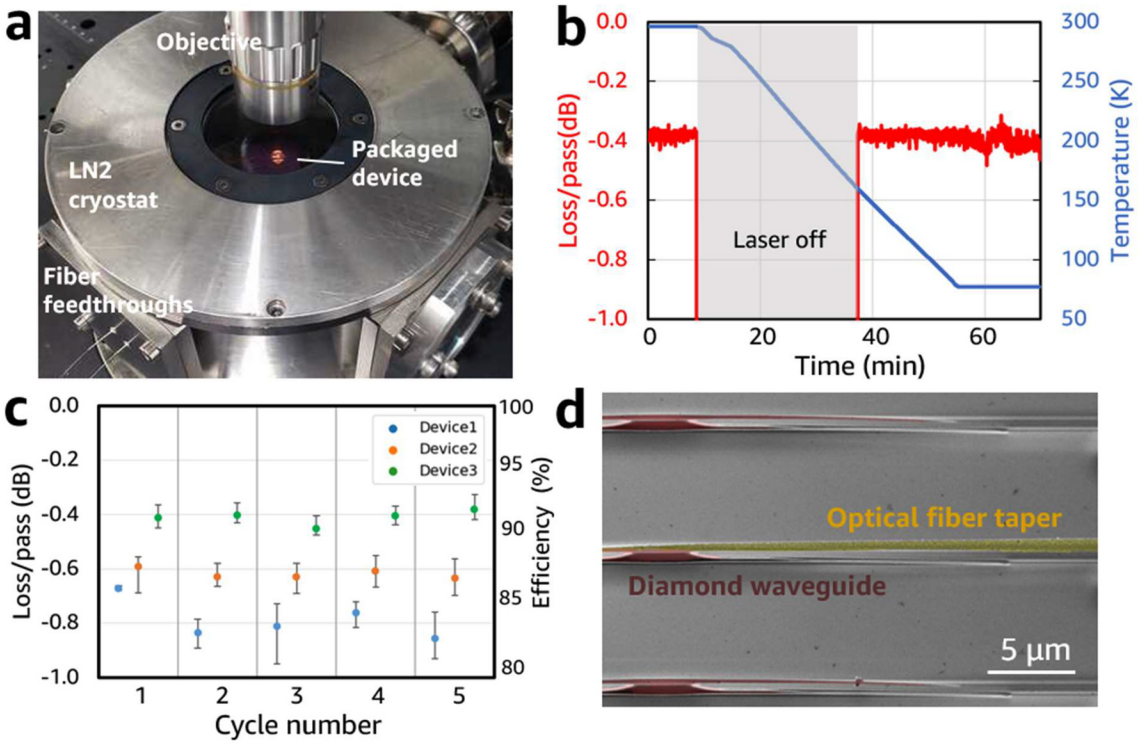

FIG. 3. (a) LN2 flow cryostat used for thermal cycling packaged samples down to 77 K. (b) Measured loss and temperature as a function of time. Laser is turned off during initial stage of cooldown to avoid optical tweezing of material outgassed from cryostat chamber. (c) Statistical losses of three packaged devices over five thermal cycles. (d) SEM image of a packaged waveguide–fiber interface after three thermal cycles showing contact between tapered fiber and tapered diamond waveguide.

this percentage, we can thus establish a lower bound of our one-way fiber-waveguide coupling efficiency of 91% or equivalently coupling loss of 0.4 dB. A small gradual decrease in coupling efficiency is observed as a result of temperature-induced stress impacting polarization of transmitted light. This can be corrected, and the ∼90% efficiency per facet can be recovered at low temperatures by changing the polarization of the input laser.

In Fig. 3(c), we document the statistical coupling loss at 77 K of three fiber-packaged devices as they pass through five thermal cycles. All samples show minimal performance degradation across five successive thermal cycles. The most heavily tested sample survived a total of more than ten cycles without any observable changes in fiber alignment or coupling efficiency. Out of five tested samples, no failure was observed during thermal cycling. Figure 3(d) shows a scanning electron microscope (SEM) image of a coupling interface after three successive thermal cycles. This confirms that the fiber taper remains firmly attached to the waveguide taper and the coupling interface is robust to the cryogenic environment.

We further demonstrate our technique's cryogenic compatibility and utility for quantum optics experiments by cooling a sample inside a dilution refrigerator and tuning the optical resonances of photonic crystal cavities inside the waveguide by condensing nitrogen (N_2) gas onto the device. Gas tuning provides a mechanism to dynamically tune cavity resonance wavelength to overcome any inhomogeneity between fabricated devices and target emitters. This is done by injecting N_2 gas via a copper tube in Fig. 4(a) near the fiber-packaged diamond device such that the nitrogen gas condenses on the sample surface. Deposited N_2 increases the refractive index of the device's environment and redshifts the cavity resonance. This technique redshifts all devices on the sample surface, at which point devices can be back-tuned individually by delivering high power laser via tapered fiber to locally evaporate N_2. This independent control over device resonances makes it possible to correct for fabrication imperfections and optimize each device resonance for spin–photon interactions. This experiment also demonstrates the waveguide–fiber interface's robustness to mechanical, chemical, and temperature perturbations, which occur as hot gas lands on milli-Kelvin temperature devices and is subsequently boiled off using high powered lasers.

No degradation in coupling efficiency is observed as the device cools from room temperature to sub-Kelvin temperatures. Similarly, coupling efficiency remains steady as we carry out gas tuning by condensing nitrogen on the diamond surface tuning the cavity resonance by 10 nm. To tune the cavity back, we send 60 μW of laser to the device to induce local heating and evaporate deposited nitrogen, bringing the cavity back to within 1 nm of its original wavelength while preserving the coupling efficiency and quality factor ($Q \sim 1300$) of the photonic cavity. Resonance spectra during the gas tuning experiment are summarized in Fig. 4(b). Note that the spectrum shape and background level depend largely on the polarization of light inside the fiber and device, which changes during the gas tuning process.

Finally, we test coupling to lithium niobate ridge waveguides and obtain better than −3.5 dB coupling per facet without modifying our

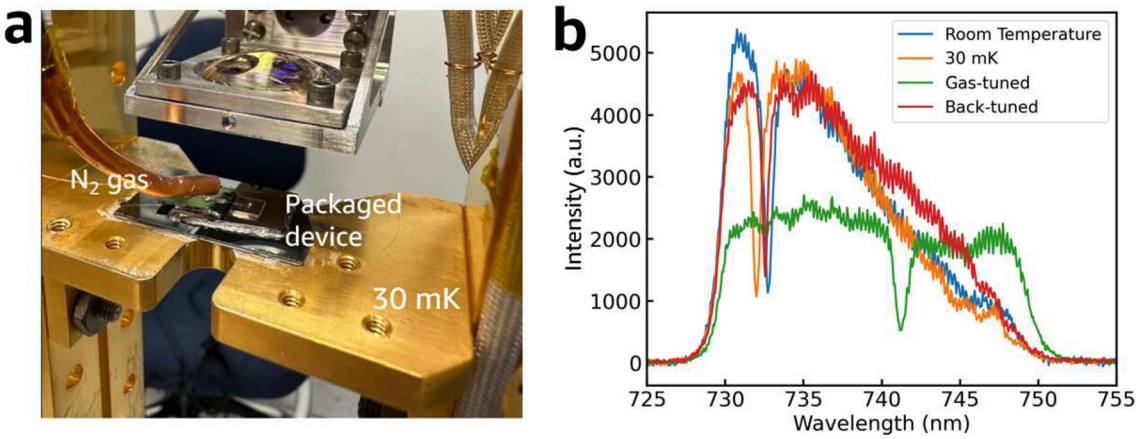

FIG. 4. (a) The packaged device with a fiber pigtail mounted in the mixing chamber of a dilution refrigerator. (b) Reflection spectra of the packaged diamond nanophotonic device at room temperature (blue), at 30 mK (orange), when gas-tuned (green) and back-tuned (red).

procedure (see the supplementary material for details). This efficiency was likely limited by the properties (e.g., fabrication errors and material degradation/oxidation) of the reflector device and the associated couplers fabricated on the lithium niobate chip and could be further improved by engineering lithium niobate geometry. Based on these results, we believe that this packaging approach could easily be adapted to operate with a wide variety of materials with low loss and thus enable a variety of devices to be used in cryogenic, remote, or otherwise hostile environments.

Efficient collection of photons from single mode waveguides operating in cryogenic environments has been an outstanding problem in the quantum-optics community for many years. The cryogenically compatible optical packaging technique demonstrated here provides an essential tool for improved performance and large-scale deployment of classical and quantum optical devices to a wide variety of challenging environments. Packaged quantum optical devices improve their individual performance and make possible the utilization of many chips inside the same cryogenic system or of multiple devices on a single chip. This is possible because the aligning and packaging processes used for this technique do not have significant chemical, optical, or mechanical crosstalk, enabling sequential or simultaneous packaging of many devices on a single substrate. Alignment can be accomplished using manually controlled micromanipulator stages—demonstrating the robustness of the technique to vibrations and small misalignment. These properties, combined with the small footprint, broad bandwidth, material agnostic nature, and high efficiency of our technique, provide incentive for its further development.

See the supplementary material for more details.

We thank Nicholas Mondrik, Antia Lamas-Linares, Oskar Painter, Simone Severini, and Bill Vass for their operational support and technical guidance and acknowledge internal funding from Amazon Web Services (AWS).

AUTHOR DECLARATIONS

Conflict of Interest

The authors have no conflicts to disclose.

Author Contributions

Beibei Zeng and Chawina De-Eknamkul contributed equally to this work.

Beibei Zeng: Conceptualization (lead); Data curation (equal); Formal analysis (equal); Investigation (lead); Methodology (lead); Project administration (equal); Resources (equal); Validation (equal); Visualization (lead); Writing – original draft (equal); Writing – review & editing (equal). **Chawina De-Eknamkul:** Data curation (equal); Formal analysis (equal); Investigation (equal); Methodology (equal); Software (lead); Validation (equal); Visualization (equal); Writing – original draft (equal); Writing – review & editing (equal). **Daniel Rimoli Assumpcao:** Data curation (equal); Formal analysis (equal); Writing – review & editing (equal). **Dylan Renaud:** Data curation (equal); Formal analysis (equal); Writing – review & editing (equal). **Zhuoxian Wang:** Methodology (equal); Validation (equal). **Daniel Riedel:** Validation (equal). **Jeonghoon Ha:** Validation (equal). **Carsten Robens:** Validation (equal); Writing – review & editing (equal). **David Levonian:** Validation (equal); Visualization (equal); Writing – review & editing (equal). **Mikhail D. Lukin:** Validation (equal); Writing – review & editing (equal). **Ralf Riedinger:** Investigation (equal); Writing – review & editing (equal). **Mihir Bhaskar:** Funding acquisition (equal); Investigation (equal); Writing – review & editing (equal). **Denis Sukachev:** Investigation (equal); Validation (equal); Writing – review & editing (equal). **Marko Loncar:** Conceptualization (equal); Resources (equal). **Bart Machielse:** Conceptualization (equal); Funding acquisition (equal); Investigation (equal); Project administration (equal); Supervision (equal); Writing – review & editing (equal).

DATA AVAILABILITY

The data that support the findings of this study are available within the article and its supplementary material.

REFERENCES

[1]D. A. B. Miller, Proc. IEEE **97**, 1166 (2009).
[2]D. D. Awschalom, H. Bernien, R. Brown *et al.*, Report No. ANL-22/83 (Argonne National Laboratory, 2022).

[3]L. P. Barry, J. Wang, C. McArdle, and D. Kilper, *Optical Switching in Next Generation Data Centers* (Springer International Publishing, 2018).
[4]R. Boyd, *Nonlinear Optics* (Academic Press, 2020).
[5]A. Sipahigil, R. E. Evans, D. D. Sukachev *et al.*, Science **354**, 847 (2016).
[6]A. W. Elshaari, W. Pernice, K. Srinivasan, O. Benson, and V. Zwiller, Nat. Photonics **14**, 285 (2020).
[7]H. J. Kimble, Nature **453**, 1023 (2008).
[8]J. Wang, S. Paesani, Y. Ding *et al.*, Science **360**, 285 (2018).
[9]J. L. O'Brien, Science **318**, 1567 (2007).
[10]C. L. Degen, F. Reinhard, and P. Cappellaro, Rev. Mod. Phys. **89**, 035002 (2017).
[11]N. Gisin and R. Thew, Nat. Photonics **1**, 165 (2007).
[12]M. Bhaskar, R. Riedinger, B. Machielse *et al.*, Nature **580**, 60 (2020).
[13]F. Arute, K. Arya, R. Babbush *et al.*, Nature **574**, 505 (2019).
[14]Y. Bian, T. Hirokawa, V. Karra *et al.*, in *Optical Fiber Communications (OFC)*, M3C.3 (2023).
[15]K. K. Mehta, C. Zhang, M. Malinowski *et al.*, Nature **586**, 533 (2020).
[16]L.-T. Feng, Y.-J. Cheng, X.-Z. Qi *et al.*, Optica **10**, 702 (2023).
[17]S. M. Meenehan, J. D. Cohen, S. Gröblacher *et al.*, Phys. Rev. A **90**, 011803 (2014).
[18]R. N. Patel, Z. Wang, W. Jiang, C. J. Sarabalis, J. T. Hill, and A. H. Safavi-Naeini, Phys. Rev. Lett. **121**, 040501 (2018).
[19]R. Riedinger, A. Wallucks, I. Marinkovic, C. Löschnauer, M. Aspelmeyer, S. Hong, and S. Gröblacher, Nature **556**, 473 (2018).
[20]D. J. Starling, K. Shtyrkova, I. Christen *et al.*, Phys. Rev. Appl. **19**, 064028 (2023).
[21]J. M. Shainline, S. M. Buckley, N. Nader, C. M. Gentry, K. C. Cossel, J. W. Cleary, M. Popovic, N. R. Newbury, S. W. Nam, and R. P. Mirin, Opt. Express **25**, 10322 (2017).
[22]T. P. McKenna, R. N. Patel, J. D. Witmer, R. Van Laer, J. A. Valery, and A. H. Safavi-Naeini, Opt. Express **27**, 28782 (2019).
[23]W. W. Wasserman, R. A. Harrison, G. I. Harris, A. Sawadsky, Y. L. Sfendla, W. P. Bowen, and C. G. Baker, Opt. Express **30**, 30822 (2022).
[24]T. G. Tiecke, K. P. Nayak, J. D. Thompson, T. Peyronel, N. P. de Leon, V. Vuletić, and M. D. Lukin, Optica **2**, 70 (2015).
[25]M. J. Burek, C. Meuwly, R. E. Evans *et al.*, Phys. Rev. Appl. **8**, 024026 (2017).
[26]P.-J. Stas, Y. Q. Huan, B. Machielse *et al.*, Science **378**, 557–560 (2022).
[27]C. T. Nguyen, D. D. Sukachev, M. K. Bhaskar *et al.*, Phys. Rev. Lett. **123**, 183602 (2019).
[28]W. Wang, H. Liu, R. Huang *et al.*, Front. Chem. **6**, 72 (2018).